i-Mechanica Journal Club for July 2019:
Cohesive strength, interfacial toughness, and their roles in the adhesion of ice

Abstract
We have recently published an article on the delamination of ice [1]. From the perspective of the ice community, this paper is significant because it introduces the notion that design of ice-resistant coatings can require consideration of the interfacial toughness between the coating and ice, rather than the interfacial strength that is traditionally considered by the community. From the perspective of the mechanics community, trained to think in terms of fracture mechanics, the paper is significant because it reminds one of the transition between conditions when the failure of interfaces is controlled by cohesive strength, and when it is controlled by interfacial toughness.

The approach described in this paper is rooted in a cohesive-zone understanding of fracture, which incorporates both strength and toughness parameters. An analysis from this perspective shows that there is a critical length of bonded interface below which strength controls delamination, and above which toughness controls delamination. Experimental observations on the delamination of ice from various coatings illustrate this transition, and reveal situations where it is either control of interfacial strength or of toughness that affects the ease with which ice can be shed from a coating.

Theoretical background
The concept that there is a transition between toughness-controlled delamination and strength-controlled delamination can be illustrated by means of a simple shear-lag analysis given in the supplemental information of Ref. [1]. Consider the geometry shown in Fig. 1, where a coating of length L, thickness h, and modulus $\bar{E}$ is bonded to a rigid substrate through a cohesive zone, and is loaded on one end by a compressive load, P.

In the following analysis, we assume that the mode-II traction-separation law is of a Dugdale form, with a shear strength of $\hat{\tau}$, toughness Γ, and critical displacement $\delta_t^* = \Gamma/\hat{\tau}$. The mode-I traction-separation law is assumed to be a delta function with a sufficiently high toughness for it not to affect the mixed-mode fracture. The analysis proceeds by considering equilibrium of a small element of length δx located at a distance x ahead of the corner (Fig. 1):

$$h\frac{\partial \sigma(x)}{\partial x} = -\hat{\tau} \ . \tag{1}$$

i-Mechanica Journal Club for July 2019: Cohesive strength, interfacial toughness, and their roles in the adhesion of ice

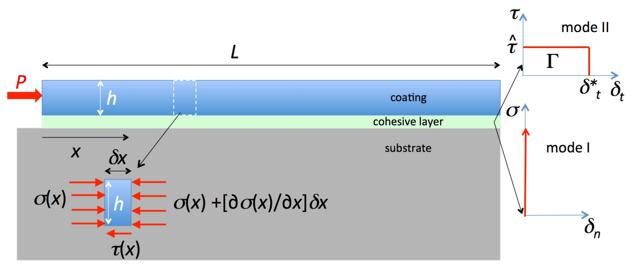

Figure 1: A shear-lag analysis can be used to explore the delamination of a coating of thickness h, length L and modulus $\bar{E}$ bonded to a thick substrate by a cohesive layer. A compressive force P (per unit width) is applied until the critical shear displacement, δ_s^* is reached.

Assuming that the coating is under uniform compression, the constitutive equation relating the stress in the coating to the local relative displacement across the interface is given by

$$\sigma(x) = -\bar{E}\frac{\partial \delta_t(x)}{\partial x} \ . \tag{2}$$

Provided the bonded length of the coating, L, is greater than the slip length $l_s = P/\hat{\tau}$, these two equations give the result

$$\frac{\partial^2 \delta_t(x)}{\partial x^2} = \frac{\hat{\tau}}{\bar{E}h} \ . \tag{3}$$

for $x < l_s$, and $\delta_t(x) = 0$ for $x > l_s$ (since a rigid substrate is assumed). There are two limiting conditions for the load. The first is that the slip zone reaches the end of the bonded interface ($l_s = L$), so equilibrium can no longer be maintained. This gives a value for the critical debond load of

$$P_f = \hat{\tau}L \ . \tag{4}$$

The second is that, before this limit is reached, the relative displacement across the interface reaches $\delta_t^* = \Gamma/\hat{\tau}$. This gives a value for the critical debond load of

$$P_f = \sqrt{2\Gamma E h} \ . \tag{5}$$

These two results can be summarized as a plot of how the delamination load varies with ligament length, L, as shown in Fig. 2. In particular, a

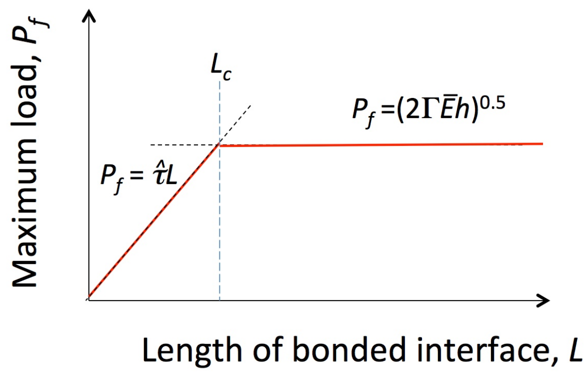

Figure 2: A transition between strength-controlled delamination and toughness-controlled delamination occurs at a critical bonding length of L_c.

comparison between Eqs. 4 and 5 indicates that there is a critical value of L at which a transition occurs between the two modes of failure:

$$L_c = \sqrt{\frac{2\Gamma\bar{E}h}{\hat{\tau}^2}} \,. \tag{6}$$

If $L < L_c$, delamination is controlled by the cohesive strength of the interface, and the load required for failure increases linearly with L. If $L > L_c$, delamination is controlled by the toughness of the interface, and the load required for failure is independent of L. It should be noted that this toughness-controlled limit is the classic linear-elastic-fracture-mechanics (LEFM) result for debonding of a coating, which can be derived by a steady-state energy balance [2, 3, 4]. This result is valid, even in the absence of a initial flaw, provided the fracture length, defined as

$$\zeta = 2\bar{E}\Gamma/\hat{\tau}^2 \,, \tag{7}$$

for a rigid substrate [5, 7], is greater than about 10% of the coating thickness [8], to give sufficient flaw-tolerance for such a geometry [6]. The transition length can be expressed as a function of the cohesive length as $L_c = \sqrt{\zeta h}$.

Previous experimental examples of the failure transition

Although, the primary intent of this article is to high-light recent work on the delamination of ice that graphically illustrates the concept of a transition

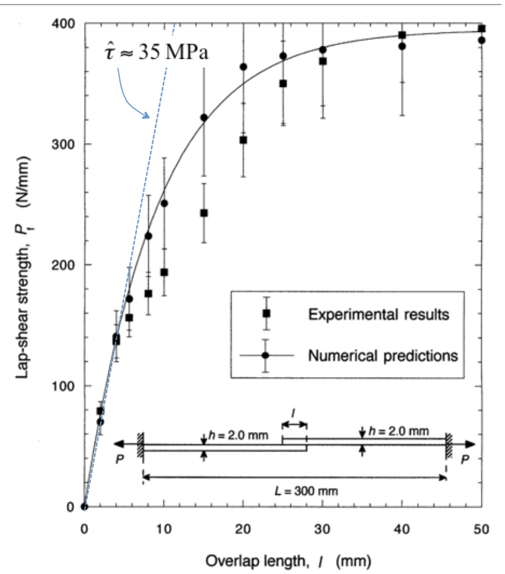

Figure 3: Experimental results and cohesive-zone predictions for an adhesively-bonded lap-shear geometry with aluminum adherends, showing how the initial slope of the plot is given by the shear strength of the adhesive. This figure has been reproduced with a minor modifications from one of the author's papers [9].

length between strength-controlled and toughness-controlled delamination, it may be of interest to remind readers of other examples where this effect has been seen, even if not specifically called out in the original publications. The first example in Fig. 3 shows the results of a lap-shear test conducted on an adhesive joint with short ligaments, from seventeen years ago [9]. As can be seen in that figure, the bond strength is initially proportional to the bond length, before it starts to plateau. It was recently noted by the author that the apparent shear strength of 35 MPa in the proportional regime is essentially identical to the value that had been used in the cohesive-zone model at the time, and which had been derived in an independent experiment [10]. The limiting value for long ligaments, although predicted correctly by the cohesive-zone model, cannot be stated analytically because of plastic deformation in the aluminum, and a combination of axial loads and bending moments.

A second example of the transition between strength-controlled fracture and toughness-controlled fracture, not commented upon at the time, is provided by an even older example, from three decades ago [11]. In this study, a long copper rod of radius 3.2 mm was embedded to a length of about 70 mm in an epoxy cylinder of radius 25 mm. When a tensile force was applied to the rod under displacement-control, a crack was driven all the way along the epoxy-copper interface. After this initial delamination along the entire interface, the rod proceeded to slip out of the epoxy under stick-slip conditions, but at an approximately constant load of 300 N, until only a few millimeters remained embedded in the epoxy. From then on, the rod was steadily pulled out of the epoxy at a load that decreased linearly with embedded length. These results are shown in Fig. 4.

At the time the paper was published, the strength controlled regime was noted upon, with the shear strength being calculated as 1.4 MPa. What was not appreciated was that the steady-state portion indicated frictional sliding of a debonded interface under toughness control. A steady-state energy balance for this geometry indicates that the failure load for propagation of a crack is given by

$$\frac{P_f}{\pi R_f^2 \bar{E}_f} = 2\sqrt{\frac{\Gamma}{\bar{E}_f R_f}} f\left(\bar{E}_m/\bar{E}_f, R_m/R_f\right) \ , \qquad (8)$$

where

$$f\left(\bar{E}_m/\bar{E}_f, R_m/R_f\right) = \left\{ \frac{1 + \left(\bar{E}_m/\bar{E}_f\right)\left[\left(R_m/R_f\right)^2 - 1\right]}{\left(\bar{E}_m/\bar{E}_f\right)\left[\left(R_m/R_f\right)^2 - 1\right]} \right\}^{0.5} \ , \qquad (9)$$

$\bar{E}_f$ and $\bar{E}_m$ are the moduli of the rod and cylinder, and R_f and R_m are the radii of the rod and cylinder. The strength-controlled failure load is given by $P_f = 2\pi R_f L \hat{\tau}$, allowing the transition length to be established.

Assuming values of $\bar{E}_f = 115$ GPa and $\bar{E}_f = 1.5$ GPa, and an average pull-out load of 300 N, one obtains a value for the toughness of the debonded interface of about 0.25 Jm^{-2}, compared with about 4 Jm^{-2} for the bonded interface. Although debonded, the interface retained structural integrity, perhaps because of a slight thermal expansion mismatch. Presumably, the

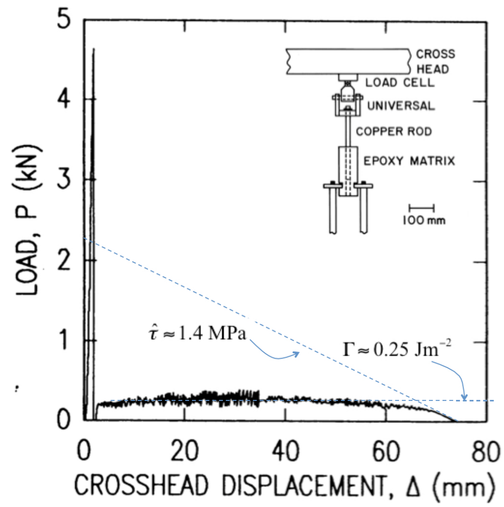

Figure 4: Load versus displacement for a debonded copper rod being pulled out of an epoxy cylinder, showing the two regimes of toughness-controlled failure and strength-controlled failure. This figure has been reproduced with minor modifications from one of the author's papers [11].

interface was sliding against friction, but it is a rather fascinating notion that this frictional interface can be characterized by a cohesive strength of 1.4 MPa and a toughness not inconsistent with a level approximating what one might expect from van der Waals bonding. It certainly supports the concept that friction can be modelled in a similar fashion to fracture by means of a cohesive-zone model [12].[1]

Debonding of Ice

With the previous examples taken from the author's prior work, accompanied by the more recent insight that was derived by the present work on ice, we can now turn our attention to the problem that raised this issue in the first place: debonding of ice. A couple of years ago, two of the co-authors of the present work developed a class of coatings having very low values of

[1] It this context it should be noted that the stick-slip portion of the pull-out probably can't be explained by a simple mode-I loss of contact caused by a Poisson's ratio contraction. An axial load of 300 N would result in a radial shrinkage of only 80 nm; a thermal expansion mismatch this small is not consistent with a frictional stress of 1.4 MPa, if Coulomb friction resulting from a misfit strain across the interface is assumed.

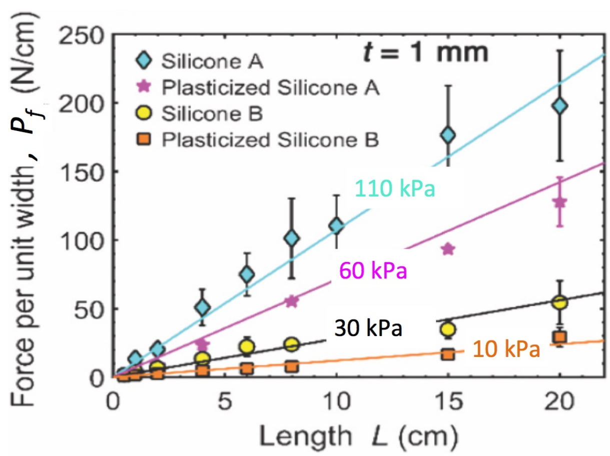

Figure 5: The cohesive strength of an interface can be measured from a plot of the force required to debond varying lengths of ice from a coating. All the coatings in this figure were 1 mm thick on aluminum, with 6 mm of ice. This figure has been reproduced with minor modifications from [1].

cohesive strength, down near 10 kPa [13]. These low cohesive strengths represented a great advance in the field, impressive for their low magnitude, given that good ice-phobic coatings are generally regarded as those materials that provide a cohesive strength of less than about 100 kPa (at least an order of magnitude less than the value obtained for uncoated aluminum surfaces.)

Consistent with common practice in the ice-community, the measurements were obtained using a standard geometry of ice, with a bonded area of about 10 mm by 10 mm. If the quoted ice-adhesion strengths represented a true cohesive strength, then the force required to push the ice off the coating would be expected to increase with bonded area. This is indeed the case, as shown in Fig. 5 for a series of coated aluminum exhibiting a range of cohesive strengths between 110 kPa and 10 kPa.

As discussed in the introduction, a transition between strength-controlled and toughness-controlled delamination is expected when the interface is long enough. Examples of this behavior are shown in Fig. 6. Both the strength and the toughness of the interface can be obtained using Eqns. 4 and 5, and

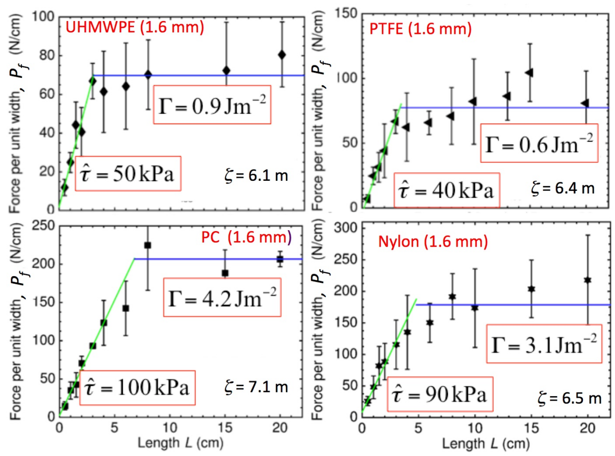

Figure 6: As the length of an interface is increased, there is a transition between strength-controlled delamination and toughness-controlled delamination, shown here for four different examples of coatings on aluminum, each of thickness 1.6 mm. The ice layer was 6 mm thick. This figure has been reproduced with minor modifications from [1].

are indicated on the plots in that figure. Additionally, the fracture length, ζ, can be calculated from Eqn. 7, with the values added to each plot. All of these examples have values of ζ between 6.1 and 7.1 m, based on the moduli of ice and aluminum. With a Dugdale cohesive law, this would correspond to a transition length of about 10 cm, compared to an actual transition length of between 3 and 7 cm. This small discrepancy probably reflects the approximations inherent in both the choices for the traction-separation law, and the assumption of a rigid substrate for the analytical model.

One of the practical implications of the transition between strength-controlled and toughness-controlled adhesion is the fact that design protocols will depend on the scale of the application. If one is interested in low adhesion at small scales, then the focus should be on low cohesive strength. If one is interested in low adhesion at large scales then the focus should be on low interfacial toughness. In particular, one needs to be aware that a system that may perform well at small scales may perform much worse at large scales than a system that performs poorly at small scales. This is illustrated by Fig. 7, which shows how a polypropylene coating with a high cohesive strength and

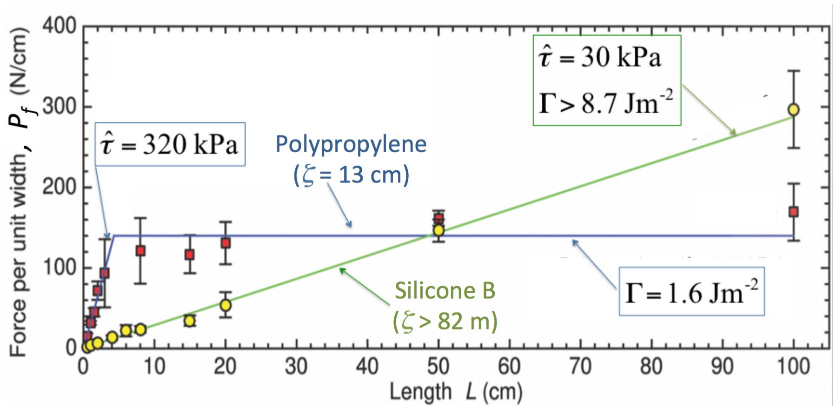

Figure 7: A coating with a low cohesive strength may can perform much more poorly at large scales than a coating with a high cohesive strength but a low toughness. The thickness of the polypropylene coating was 1.58 mm; the thickness of the silicone B coating was 1 mm. The thickness of the ice was 6 mm. This figure has been reproduced with minor modifications from [1].

a relatively low toughness, requires about half the force to debond a meter of ice than does a silicone coating with a relatively low cohesive strength and a high toughness.

As explained in Ref. [1], the design of low-toughness coatings provides another example of the use of a cohesive-zone approach to fracture. From this perspective, deformation in the coating contributes to the toughness of the coating. Therefore, one can approximate the toughness of an interface that includes the deformation of the coating within the definition of a traction-separation law by the expression

$$\Gamma = \frac{\hat{\tau}^2 t}{2G} \, , \tag{10}$$

where t is the thickness of the coating, and G is the shear modulus of the coating. A thin, stiff coating is expected to result in a low toughness. This is the opposite strategy used for low-strength coatings which tend to be thick and with a low modulus. The effect of modulus can be seen from the data of Fig. 7. The effect of thickness was illustrated in Ref. [1], as was the effect of controlling $\hat{\tau}$ on the toughness of ice-coating systems. Focusing on the thickness and cohesive strength, the authors demonstrated the development of coatings that had values of toughness approaching 0.1 Jm^{-2} [1].

Conclusions

The major concept for the mechanics community to appreciate from this work is the fact that the dual concepts of cohesive strength and interfacial toughness are important when analyzing delamination phenomena. Historically, the focus in the fracture community has been on the concept of toughness, although other communities have often focussed on strength. Cohesive-zone models of fracture allow one to appreciate the dual nature of delamination. At small length scales, the concept of cohesive strength can be more important. At large length scales, the concept of toughness becomes more important. The design of interfaces requires that both of these concepts be considered, as appropriate for the regimes in which each might be dominant.

References

[1] K. Golovin, A. Dhyani, M. D. Thouless and A. Tuteja, "Low interfacial toughness materials for effective large-scale de-icing," *Science*, **364**, 371-375 (2019)

[2] K. Kendall, Shrinkage and peel strength of adhesive joints. *J. Phys. D*, **6**, 1782-1787 (1973).

[3] M. D. Thouless, A. G. Evans, M. F. Ashby and J. W. Hutchinson, "The edge cracking and spalling of brittle plates," *Acta Metall.*, **35**, 1333-1341 (1987).

[4] Z. Suo and J. W. Hutchinson, "Interface crack between two elastic layers," *Int. J. Fract.*, **43**, 1-18 (1990).

[5] A. Hillerborg, M. Modéer, P.-E. Petersson, "Analysis of crack formation and crack growth in concrete by means of fracture mechanics and finite elements," *Cement Conc. Res.*, **6**, 773-781 (1976).

[6] G. Bao and Z. Suo, "Remarks on crack-bridging concepts," *Appl. Mech. Rev.*, **45**, 355–366 (1992).

[7] R. B. Sills and M. D. Thouless "The effect of cohesive-law parameters on mixed-mode fracture," *Eng. Fract. Mechs.*, **109**, 353-368 (2013).

[8] J. M. Gorman and M. D. Thouless,"When do corners behave like cracks," manuscript in preparation (2019).

[9] M. S. Kafkaldis and M. D. Thouless,"The effects of geometry and material properties on the fracture of single lap-shear joints," *Int. J. Sol. Structs.*, **39**, 4367-4383 (2002).

[10] Q. D. Yang, M. D. Thouless and S. M. Ward, "Elastic-plastic mode-II fracture of adhesive joints," *Int. J. Sol. Structs.*, **38**, 3251-3262 (2001).

[11] R. F. Cook, M. D. Thouless, D. R. Clarke and M. C. Kroll, "Stick-slip during fibre pull-out," *Scripta Metall.*, **23**, 1725-1730 (1989).

[12] Z. Hu, W. Lu and M. D. Thouless, "Slip and wear at a corner with Coulomb friction and an interfacial strength" *Wear*, **338-339**, 242-251 (2015).

[13] K. Golovin and A. Tuteja, "A predictive framework for the design and fabrication of icephobic polymers," *Science Advances*, **3**, e1701617 (2017).